KSME

Springer

Journal of Mechanical Science and Technology 34 (12) 2020

Original Article
DOI 10.1007/s12206-020-1121-4

Keywords:
· Five-boundary condition forming angle distribution function (FAI.5B)
· Forming angle
· Roll forming
· Springback

Correspondence to:
Longyun Yang
yanglongyun2016@163.com

Citation:
Su, C., Liu, J., Zhao, Z., Lou, S., Wang, R., Yang, L. (2020). Research on roll forming process and springback based on five-boundary condition forming angle distribution function. Journal of Mechanical Science and Technology 34 (12) (2020) 5193~5204.
http://doi.org/10.1007/s12206-020-1121-4

Received August 27th, 2019
Revised August 6th, 2020
Accepted September 2nd, 2020

† Recommended by Editor Hyung Wook Park

Research on roll forming process and springback based on five-boundary condition forming angle distribution function

Chunjian Su, Jiazhen Liu, Zexuan Zhao, Shumei Lou, Rui Wang and Longyun Yang

College of Mechanical and Electronic Engineering, Shandong University of Science and Technology, Qingdao 266590, China

Abstract In the present study, a five-boundary conditional distribution function of the forming angle is proposed. The stress, strain, and springback of a sheet in roll-forming process under three different angle distribution functions are studied. Furthermore, effects of forming angle increment, sheet thickness, and material yield strength on stress, strain distribution, and springback of sheet during roll forming are studied under optimized forming angle. The results demonstrate that stress, strain, and springback of each pass based on increment of forming angle under five-boundary condition during roll forming are less than those achieved by other forming angle distribution methods. The stress and strain in the bending zone increase with increase in the sheet thickness. After roll forming, the springback angle decreases with the increase of sheet thickness, increases with the increase of forming angle and material yield strength. However, springback angle can be effectively reduced by increasing the number of passes or correction rolls.

1. Introduction

Roll forming is a continuous, efficient, and high-quality metal profile forming technology for making a sheet of a certain size bend transversely under the action of forming rolls in multiple passes to obtain its specified cross-sectional shape [1]. The work process of roll forming is illustrated in Fig. 1. In particular, the sheet is bent to a desired shape through the upper and lower forming rolls of different shapes arranged in sequence [2, 3]. This technology is currently widely used in construction, automobile manufacturing, aerospace, and other fields [4, 5].

The forming angle is the most important technological parameter in the roll-forming process. The distribution of bending determines the shape of the rolls and forming of the sheet [6]. At present, there is no strict theory defining the division of the forming angle, which thus relies on the production experience. Therefore, a complete and effective method for dividing the forming angle reasonably in the roll forming process is required [7, 8]. A Japanese scholar Ona and other researchers [9] have suggested that the edge deformation of a sheet follows a cubic curve and explored the problems associated with the forming pass and forming angle distribution in the roll-forming process. The study demonstrated that the horizontal projection track of the vertical edge follows a cubic curve allowing to achieve a desirable forming angle distribution. Bidabadi et al. [10, 11] studied the longitudinal bowing of symmetric U-channel sections in roll forming by means of finite element simulation and experiments, the results demonstrated that the most important forming parameters are forming angle increment. Han et al. [12] established a B3-spline finite strip method to study the effect of forming parameters on roll forming, the results demonstrated that the peak longitudinal edge film strain increases with the increase of forming angle.

However, springback is a common product defect in the production process of mechanical processing, which greatly affects the accuracy and quality of products [13]. Weiss et al. [14]

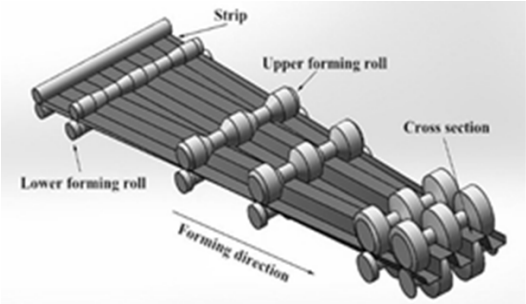

Fig. 1. Roll forming process.

compared the springback of roll forming and V-shaped forming. The product quality under roll forming is obviously better than that under V-shaped forming. Groche et al. [15] developed a closed-loop calibration system for springback during forming and integrated it into conventional forming lines to improve the geometric accuracy of profiles and compensate for the deviation caused by springback. Zeng et al. [16] used the response surface method to determine the increment of the forming angle, reduce springback and peak longitudinal strain, and optimized using the springback angle as an objective function and maximum longitudinal strain of the edge film as a constraint condition. The forming accuracy was improved successfully, and the defects of the product edge wave were eliminated.

Prior to the study presented in this paper, based on our practical production experience and theoretical analysis, we successfully put forward a forming angle distribution function based on the five-boundary condition and constructed a curve equation for the projection trajectory of the contour section edge in the horizontal plane [17]. At the same time, another study proved that the forming angle distribution is the best when the forming angle of the first third of the forming passes is $\theta_{N/3} = 33\,\% \times \theta_0$ [13]. In this paper, the five-boundary conditional distribution function of the forming angle is proposed, and then the effects of forming angle distribution, material yield strength and sheet thickness on the angle distribution and springback of strain in roll forming process are studied.

2. Methodologies

2.1 Roll forming theory based on five-boundary condition forming angle distribution function

2.1.1 Forming angle distribution based on four-boundary condition forming angle distribution function

Estimating the forming angle is the most important and difficult problem in the roll forming design. A reasonable distribution of the forming angle can alleviate the stress concentration and resulting defects such as longitudinal bending, corner tearing, and springback. According to the production experience and related theory, Japanese scholar Ona et al. [9] proposed a distribution formula of the forming angle in roll forming. It is assumed that the distribution of the forming angle of a sheet is the best when the projection trajectory of the horizontal plane at the end of the vertical edge follows a cubic curve. The process of deriving the forming angle distribution is illustrated in Fig. 2.

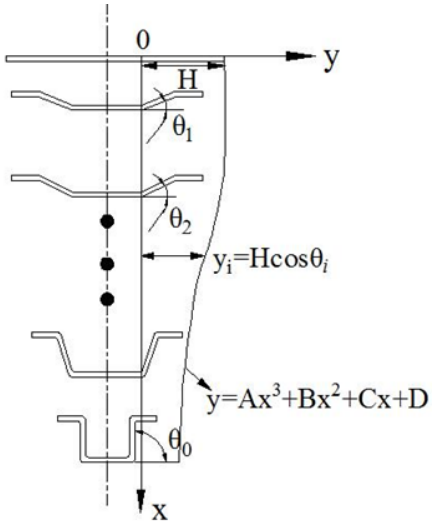

Fig. 2. Projection track of the edge of a hat-shaped steel section in the horizontal plane.

In the forming process of hat-shaped parts shown in Fig. 2, assuming that the number of forming passes is N, the final forming angle of the vertical edge is θ_0, the length of the vertical edge is H, and the forming angle of the vertical edge of the first pass is θ_i, the expression of the cubic curve is as follows:

$$y = Ax^3 + Bx^2 + Cx + D. \tag{1}$$

The four boundary conditions are as follows:

$$\begin{cases} \dfrac{dy}{dx} = 0, (x = 0) \\ \dfrac{dy}{dx} = 0, (x = N) \\ y = H, (x = 0) \\ y = H\cos\theta_0, (x = N). \end{cases} \tag{2}$$

Combining Eqs. (1) and (2), the following Eq. (3) can be obtained:

$$\begin{cases} C = 0, (x = 0) \\ 3AN^2 + 2BN + C = 0, (x = N) \\ D = H, (x = 0) \\ AN^3 + BN^2 + CN + D = H\cos\theta_0, (x = N). \end{cases} \tag{3}$$

According to Eq. (3), the coefficients of the cubic curves A, B, C, and D can be calculated as

Table 1. Forming angle distribution of the four-boundary condition.

Forming passes number									
i	1	2	3	4	5	6	7	8	9
θ_i	15.0	29.1	42.2	54.3	65.4	75.0	82.7	88.0	90.0
$\Delta\theta_i$	15.0	14.1	13.1	12.1	11.1	9.6	7.7	5.3	2.0

$$\begin{cases} A = \dfrac{2H(1-\cos\theta_0)}{N^3} \\ B = \dfrac{3H(\cos\theta_0 - 1)}{N^2} \\ C = 0 \\ D = H. \end{cases} \tag{4}$$

Therefore, Eq. (1) can be rewritten as

$$y = \frac{2H(1-\cos\theta_0)}{N^3}x^3 + \frac{3H(\cos\theta_0 - 1)}{N^2}x^2 + H. \tag{5}$$

When $x = i$ and $y_i = H\cos\theta_i$, the relationship between the forming angle and forming pass in Eq. (5) can be written as

$$H\cos\theta_i = \frac{2H(1-\cos\theta_0)}{N^3}i^3 + \frac{3H(\cos\theta_0 - 1)}{N^2}i^2 + H. \tag{6}$$

Thus, a further simplification can be obtained by expressing the *i* roll forming pass for the forming angle θ_i as

$$\cos\theta_i = 1 + (1-\cos\theta_0)\left[2\left(\frac{i}{N}\right)^3 - 3\left(\frac{i}{N}\right)^2\right]. \tag{7}$$

The forming angle of each forming pass can be calculated for $i = 1,2,3\ldots N$ using Eq. (7). The four-boundary conditional forming angle distribution of nine forming passes is shown in Table 1, where i denotes the forming pass number, θ_i denotes the forming angle, and $\Delta\theta_i$ denotes the forming angle increment.

2.1.2 Forming angle distribution based on five-boundary condition forming angle distribution function

The method for obtaining the forming angle distribution based on the four-boundary conditional forming angle distribution function has some regularity, which makes the distribution of the forming angle quantitative. However, it cannot guarantee an optimal distribution result, and there are some limitations. According to the actual production experience and theoretical statistical analysis, the forming angle of the first third pass in the roll-forming process does not exceed 50 % of the final forming angle in most cases, that is, $\theta_{N/3} \le 50\,\% \times \theta_0$ [13]. Accordingly, the fifth boundary condition can be assumed for the four-boundary condition forming angle distribution function, that is, $y_{N/3} = H\cos\theta_{N/3}$. Combining this boundary condition with the four-boundary conditions of Eq. (2), a forming angle distribution function based on five-boundary conditions can be constructed.

Assuming that the projection trajectory of the horizontal plane at the end of the vertical edge of the profile section is part of the quadric curve, the expression of the quartic curve can be written as

$$y = Ax^4 + Bx^3 + Cx^2 + Dx + E. \tag{8}$$

When $x = N/3$ and $y = H\cos\theta_{N/3}$, the five-boundary conditions of Eq. (8) are:

$$\begin{cases} \dfrac{dy}{dx} = 0, (x = 0) \\ \dfrac{dy}{dx} = 0, (x = N) \\ y = H\cos\theta_{N/3}, (x = N/3) \\ y = H, (x = 0) \\ y = H\cos\theta_0, (x = N). \end{cases} \tag{9}$$

When $x = i$ and $y_i = H\cos\theta_i$, according to the derivation process of the four-boundary conditional forming angle distribution function combined with Eqs. (8) and (9), the forming angle θ_i of the *i* pass in roll forming can be obtained based on the five-boundary conditional forming angle distribution function as:

$$\cos\theta_i = 1 + \frac{81\cos\theta_{N/3} - 60}{4N^4}i^4 + \frac{-81\cos\theta_{N/3} + 64}{2N^3}i^3 + \frac{81\cos\theta_{N/3} - 72}{4N^2}i^2. \tag{10}$$

According to the previous study [10], the optimal interval of the first third pass forming angle is $30\,\% \times \theta_0 \le \theta_{N/3} \le 35\,\% \times \theta_0$, and $\theta_{N/3} = 33\,\% \times \theta_0$ is selected in this study. The result of the forming angle distribution of the corresponding pass can then be obtained according to Eq. (10) for $i = 1,2\ldots 9$, as shown in Table 2. The roll-forming parameters and their symbols adopted in this study are listed in Table 3.

2.2 Finite element simulation

We used ABAQUS software to simulate the roll-forming process of two sheets. The mechanical properties of the sheets are listed in Table 4, while the true stress-strain curves are shown in Figs. 3 and 4 illustrates the finite element model of roll forming, in which the mesh of a sheet is divided as demonstrated in

Table 2. Forming angle distribution for each pass of 33 %×θ_0 .

$\theta_{N/3}$	Forming pass number									
33 %×θ_N	i	1	2	3	4	5	6	7	8	9
	θ_i	7.7	18	29.7	42.2	54.9	67.2	78.3	86.6	90
	$\Delta\theta_i$	7.7	10.3	11.7	12.5	12.7	12.3	11.0	8.3	3.4

Table 3. Table of roll forming parameters and symbols.

Roll forming parameters	Symbols
Forming angle increment (distribution method)	FAI
Five-boundary condition forming angle distribution function	FAI.5B
Four-boundary condition forming angle distribution function	FAI.4B
10° increment of forming angle	FAI.10°
Sheet thickness	S.T.
Equivalent plastic strain	PEEQ
Stress	S

Table 4. Mechanical properties of sheets.

Sheets	Young's modulus (GPa)	Mass density (kg/m^3)	Yield limit (MPa)	Poisson's ratio	Ultimate strength (MPa)
Q235	212	7.86E+03	235	0.288	450
DP780	218	8.0E+03	578	0.3	886

Table 5. Main parameters of roll forming machine in experiments.

Forming parameters	Forming speed (m/min)	Motor power (Kw)	Roller distances (mm)	Forming passes
Value	5–10	7.5	500	9

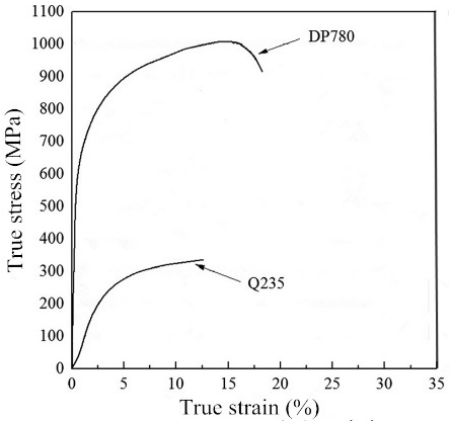

Fig. 3. True stress-strain curve.

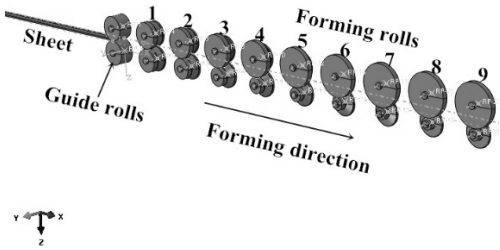

Fig. 4. Finite element model of roll forming.

Fig. 5. The mesh is refined in the bending zone to achieve more accurate simulation results.

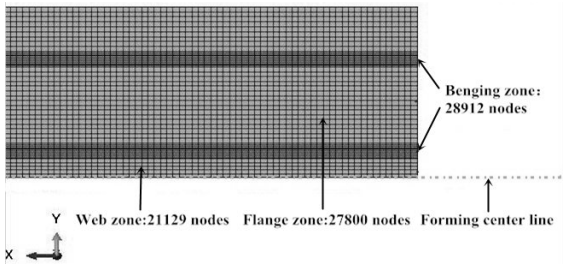

Fig. 5. Mesh division of a sheet.

2.3 Experiment

2.3.1 Roll forming process experiment

The main parameters of the roll-forming machine used in the experiment are listed in Table 5. The roll-forming machine and the experimental products are shown in Figs. 6 and 7, respectively. The mechanical properties were measured by via tensile tests, according to ASTM-E8, using a universal material testing machine. The experimental results agree with the true stress-strain curve of the material in the simulation, as shown in Fig. 3.

2.3.2 Measurement of springback angle in roll forming

Roll forming is a continuous and gradual forming process, that is, a sheet is formed using rolling at different forming angles, where the loading-unloading force is repeatedly applied to the sheet impacting its springback. In this study, the springback angle was measured in a roll-forming experiment using a universal protractor as the measuring tool. The definition of the springback measurement is shown in Fig. 8, where θ denotes the forming angle upon unloading the load after forming, θ' denotes the forming angle without unloading the load after forming, and the springback is equal to the difference between them.

Fig. 6. Roll forming machine.

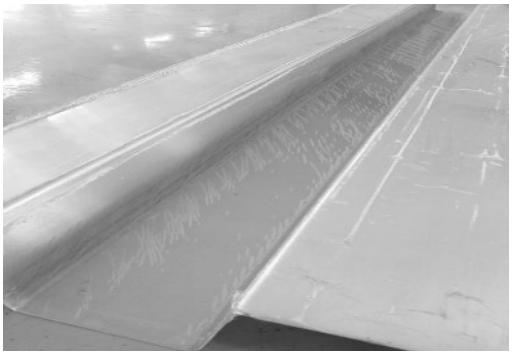

Fig. 7. Experimental products.

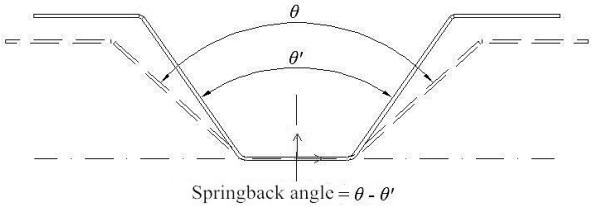

Fig. 8. Definition of springback.

3. Results and discussion

3.1 Effect of the forming parameters on sheet forming

3.1.1 Effect of forming angle distribution method on sheet forming

(1) Five-boundary condition forming angle distribution function

A Q235 sheet with a thickness of 1.5 mm was selected to simulate in this study, and the roll-forming changes were studied in the 2nd, 4th, 6th, and 9th passes. Fig. 9 shows the equivalent stress nephogram of the sheet forming process based on FAI.5B. It can be seen from the figure that the maximum forming force (about 298 MPa) of the sheet subjected to rolls is distributed mainly in the bending zone of each forming pass. However, there is also a large stress concentration in the web and zones of the 4th and 6th passes, which is due to the large increment of the forming angle. The greater the increment of

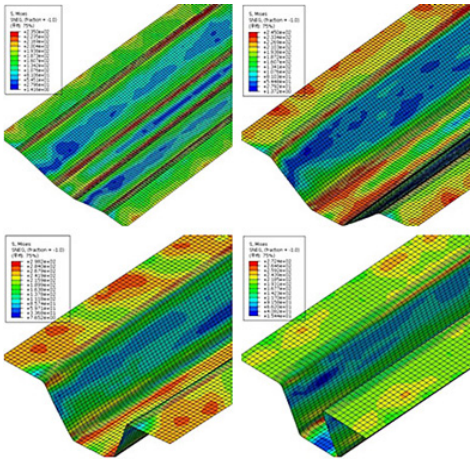

Fig. 9. Stress contour based on FAI.5B.

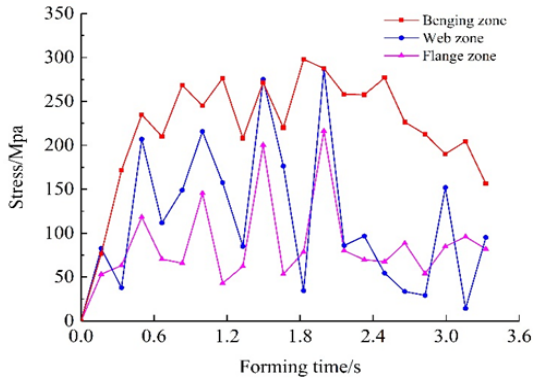

Fig. 10. Stress-history curve based on FAI.5B.

the forming angle is, the greater the stress in each area of the sheet is. When the final section is formed in the 9th pass, the stress in the bending zone exceeds the yield strength of Q235 by 235 MPa, but is much lower (by 450 MPa) than the ultimate tensile strength of the sheet, which ensures the forming accuracy of the transverse section. The maximum stress in the web and flange zones is about 219 MPa, which refers to elastic deformation. The original shape can be restored by removing the load. This confirms the rationality of the angular distribution function under FAI.5B.

Fig. 10 shows the stress evolution curve of a sheet during roll forming based on FAI.5B. It demonstrates the stress variation law of the bending, web, and flange zones. The variation of thethree broken lines in the figure indicates that the stress increases when the roll is passing through the sheet, and decreases when the roll is separated from the sheet. The stress broken lines in three different regions show that the maximum stress in the bending zone is 298 MPa per pass, followed by the stress in the web zone. The peak stress in the 5th and 6th passes is close to 300 MPa, while the stress in the other passes is stable at 200 MPa, because the greater the increment of the forming angle is, the greater the stress in the sheet is. The minimum stress occurs in the flange zone, the peak stress is close to 200 MPa at the 5th and 6th passes, while the

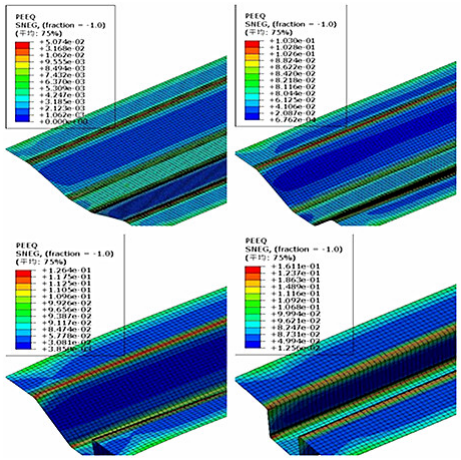

Fig. 11. Equivalent plastic strain contour based on FAI.5B.

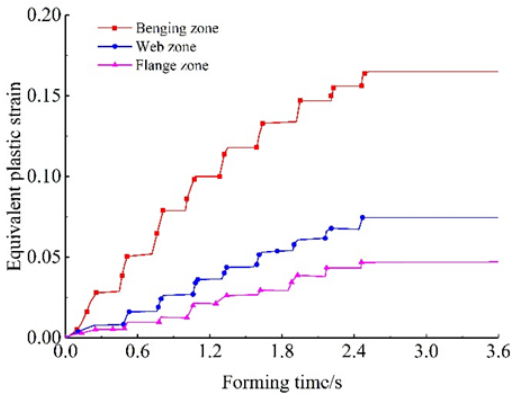

Fig. 12. Equivalent plastic strain-history curve based on FAI.5B.

peak stress of the other passes is stable at 100 MPa on average. It can also be seen that the peak stress increases with the increase in the forming angle. When the forming time is more than 2.4 s, the initial meshing part of the sheet has been formed out of the roll, but it is still affected by the following sheet forming stress. Thus, the stress in the bending, web, and flange zones still exists, and it is far lower than the yield strength of the material.

Figs. 11 and 12 show the equivalent plastic strain nephogram and equivalent plastic strain variation curve of the sheet forming process FAI.5B. It can be noticed from Fig. 11 that a part of plastic deformation also occurs at the edge of the forming part in each pass because the edge wave tends to occur at the edge of the sheet in the forming process. The maximum equivalent plastic strain of each pass occurs in the bending zone. The maximum equivalent strains of the 2nd, 4th, 6th, and 9th passes are 0.05, 0.103, 0.126, and 0.165, respectively. This confirms that the plastic strain occurs in the bending zone, which can ensure the accuracy of the roll forming parts. Fig. 12 demonstrates that the equivalent plastic strain in the bending zone is significantly higher than that in the web and flange zones. The equivalent plastic strain in the bending zone gradually accumulates to 0.165 from the 1st to 9th pass, and the

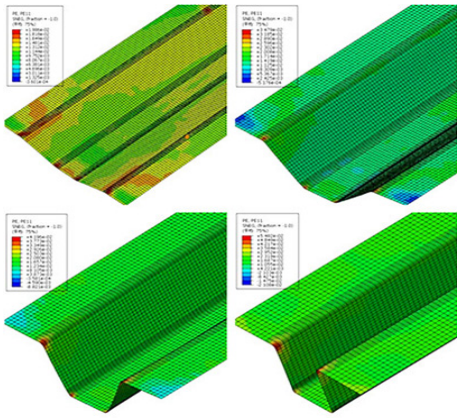

Fig. 13. Longitudinal plastic strain contour based on the FAI.5B.

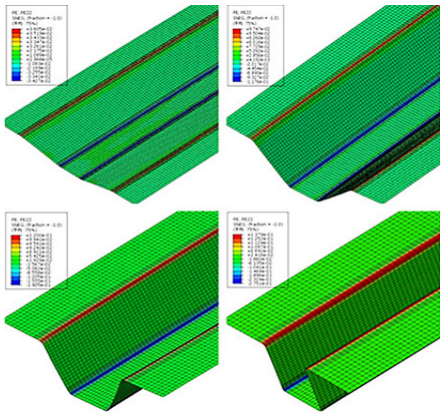

Fig. 14. Transverse plastic strain contour based on the FAI.5B.

strains in the web and flange zones accumulate to 0.075 and 0.047, respectively, indicating that different degrees of plastic strain have occurred. Fig. 12 illustrates that the plastic strain increases rapidly in the first five passes, which is closely related to the increment of the forming angle and position of the initial meshing. It also shows that the equivalent plastic strain increases with the increase in the forming angle.

Figs. 13 and 14 represent the longitudinal (length direction) and transverse (width direction) plastic strain in the roll-forming process of a sheet, respectively. The 2nd pass in Fig. 13 indicates that the whole sheet has plastic strain in varying degrees from the cloud color, while the plastic strain of the 4th, 6th, and 9th passes concentrates in the bending zone of the initial meshing of the sheet, which fully illustrates the importance of the initial meshing in sheet forming. Fig. 14 demonstrates that the plastic strain mainly occurs in the bending zone and it is becoming more serious with the increase in the forming angle, which meets the actual production requirements. To produce the required cross-section roll-forming parts, the transverse deformation is required. Fig. 15 shows a comparison between the longitudinal and transverse strain. The transverse plastic strain is greater than the longitudinal plastic strain in each pass. The transverse strain accumulates to 0.05 in the 6th pass and 0.14 in the 9th pass. The transverse strain is required for the

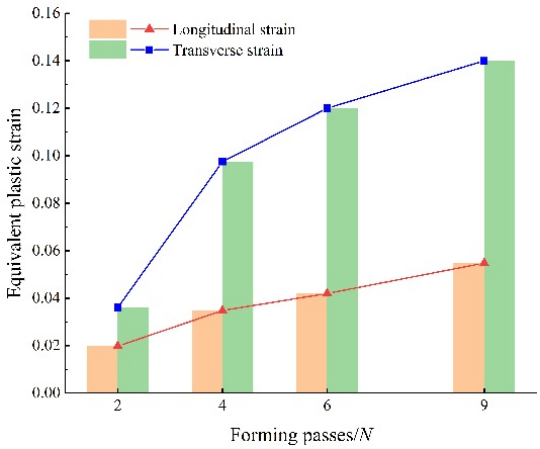

Fig. 15. Comparison between the longitudinal and transverse plastic strain based on FAI.5B.

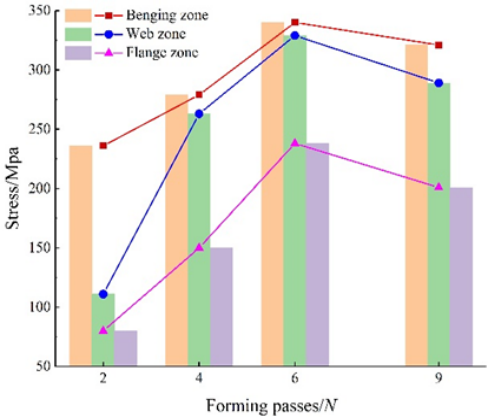

Fig. 16. Maximum stress curves for different passes based on FAI.4B.

product, whereas the longitudinal strain would cause springback and longitudinal bow shape defects. In Fig. 15, the increase in the longitudinal plastic strain is gentle, whereas the increase in the transverse plastic strain is slow and urgent, which also reflects the importance of the initial meshing of the sheet and the complexity of the roll-forming process.

(2) Four-boundary condition forming angle distribution function

Fig. 16 shows the maximum stress curve of the 2nd, 4th, 6th, and 9th passes, which reflects the stress changes in the sheet. It is obvious from the figure that the stress of each pass increases with the increase of passes, and the stress in the bending zone and the upper web zone of the sheet becomes more concentrated. In the 2nd, 4th, and 6th passes, the stress concentration appeared at the edge of the upper web, in which the stress of the 6th passes reached 340 MPa; in the 9th passes, the whole upper web showed relatively large stress, which all exceeded the yield strength of the material and caused permanent deformation, and the maximum stress reached 321 MPa. The stress in the bending zone is higher than that in the web and flange zones, and the maximum stress is close to

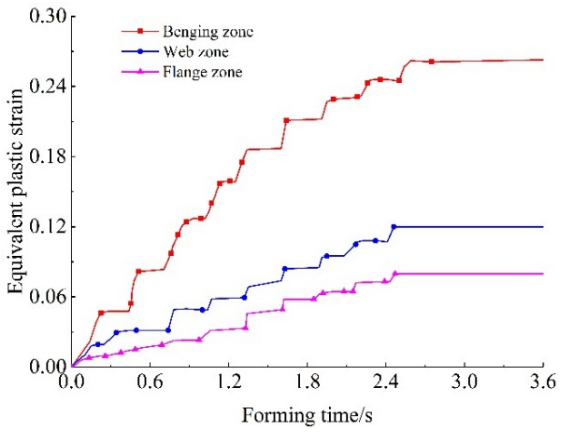

Fig. 17. Equivalent plastic strain-history curve based on FAI.4B.

350 MPa, which does not exceed the tensile limit of the material and has no risk of material rupture. The stress distribution of forming angle distribution function based on FAI.4B is basically the same as that based on FAI.5B, but the stress value is larger.

Fig. 17 shows the equivalent plastic strain curves for the bending, web, and flange zones. It can be seen from the graph that the plastic strain in the bending zone is obviously higher than that in the web and flange zones, and the cumulative equivalent plastic strain in the bending zone is 0.26 in the 9th pass. Equivalent plastic strain in web zone eventually accumulated to 0.12, and that in flange zone eventually accumulated to 0.08. Equivalent plastic strain also concentrates in the bending zone, and plastic strain also occurs at the edge of the upper web, with the same variation rule for each pass.

(3) 10° increment of the forming angle

The stress and equivalent plastic strain curves of roll forming process based on FAI.10° are shown in Figs. 18 and 19. In Fig. 19, the maximum stress in the bending, web and flange zones are similar at the 2nd, 4th, and 6th passes. The stress in the bending zone is still the largest, and increases gradually with the increase of the forming angle, and the change is uniform. In the 9th pass, the strain reaches 392 MPa, which is completely inconsistent with the stress change curve of forming angle based on FAI.5B and FAI.4B, which is the reason for the uniform increase of forming angle. In Fig. 19, the equivalent plastic strain in roll forming process of sheet is similar to that in forming angle based on FAI.5B and FAI.4B. The equivalent plastic strain in bending, web and flange zone are higher than that in forming angle distribution based on FAI.5B and FAI.4B, and the maximum effective plastic strain can be reached to 0.295.

The stress and equivalent plastic strain curves of the roll-forming process based on 10° increment of the forming angle are shown in Figs. 18 and 19, respectively. In Fig. 18, the maximum stress values in the bending, web, and flange zones are similar in the 2nd, 4th, 6th, and 9th passes. The stress in the bending zone is still the largest and increases gradually with the increase in the forming angle, and its change is uniform. In

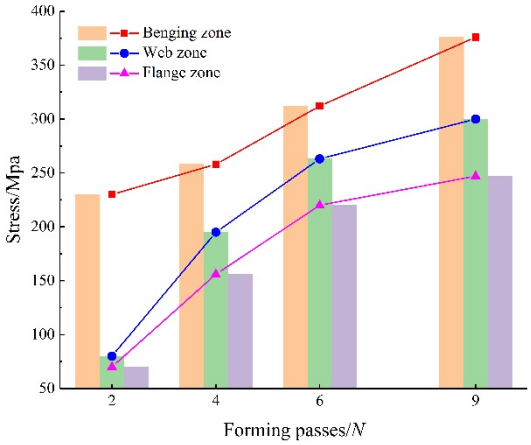

Fig. 18. Stress-history curve based on FAI.10°.

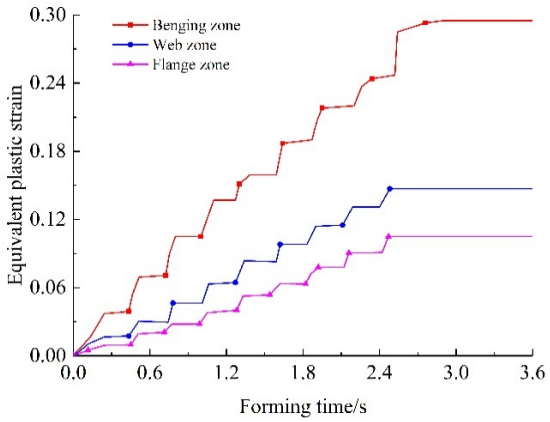

Fig. 19. Equivalent plastic strain-history curve based on FAI.10°.

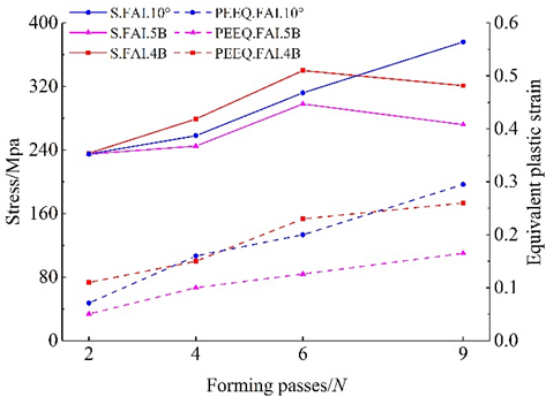

Fig. 20. Comparison of stress and equivalent plastic strain in forming zone based on different FAIs.

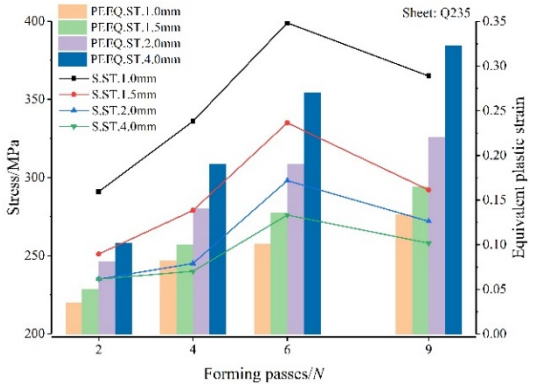

Fig. 21. Stress and equivalent plastic strain for different passes in effect of different S.T. based on FAI.5B.

the 9th pass, the strain reaches 392 MPa, which is completely inconsistent with the stress change curve of the forming angle based on FAI.5B and FAI.4B and is the reason for the uniform increase in the forming angle. In Fig. 19, the equivalent plastic strain in the roll-forming process of the sheet is similar to that based on FAI.5B and FAI.4B. The equivalent plastic strain values in the bending, web, and flange zones are higher than that based on FAI.5B and FAI.4B, while the maximum effective plastic strain can reach 0.295.

(4) Comparison of different methods for estimating the distribution of the forming angle

The maximum stress and equivalent plastic strain in the bending zone can be obtained based on the change of the stress and equivalent plastic strain curves under the impact of three different angular distribution modes, namely, FAI.5B, FAI.4B, and FAI.10°. The stress and equivalent plastic strain in the bending zone under the three modes are compared in Fig. 20.

In Fig. 20, the solid lines represent the law of the stress change, whereas the dotted lines represent the law of the equivalent plastic strain change. In the 2nd, 4th, and 6th passes, the stress of the sheet based on FAI.4B is the highest, whereas that based on FAI.5B is the lowest. In the 9th pass, the stress of the sheet based on FAI.10° reaches 376 MPa and exceeds that based on FAI.4B; however, this value does not exceed the tensile limit of the material. Moreover, the stress of the sheet based on FAI.5B is still the lowest in the 9th pass, indicating the superiority of this mode in forming. The maximum plastic strain of 0.295 occurs in the 9th pass based on FAI.10°, while the maximum equivalent plastic strain of 0.165 occurs under the condition of FAI.5B.

It can be noticed from Fig. 20 that the stress of the sheet in each FAI increases with the increase in the angle distribution function, the equivalent plastic strain of the sheet in each FAI increases with the increase in the forming angle and angle increment, and the performance of the roll-forming parts based on FAI.5B is the best.

3.1.2 Effect of sheet thickness on sheet forming

Based on FAI.5B, the effects of the sheet thickness of 1.0 mm, 1.5 mm, 2.0 mm, and 4.0 mm on the roll-forming parts were studied. The same Q235 material was used in this experiment. Fig. 21 illustrates the effect of the sheet thickness on the stress and equivalent plastic strain in the bending zone of the sheet based on FAI.5B.

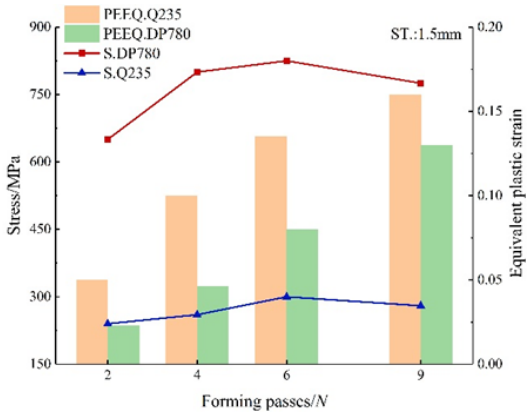

Fig. 22. DP780 stress and equivalent plastic strain for different passes based on FAI.5B.

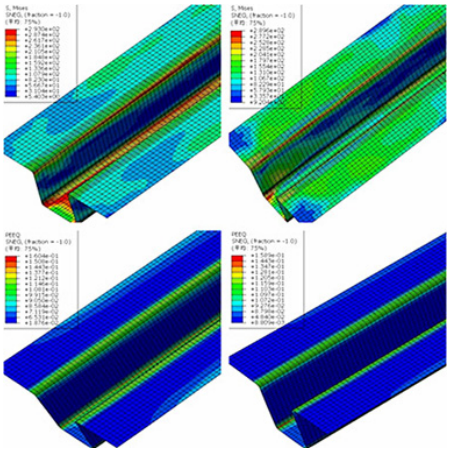

Fig. 23. Stress and strain before and after springback based on FAI.5B.

In can be noticed that there is a variation of the stress and equivalent plastic strain in the bending zone depending on the sheet thickness, while the magnitude of this variation remains the same across all passes. The stress and plastic strain in the bending zone of the sheet increase with the increase of the sheet thickness. The stress in roll forming of sheet is affected by the increment of forming angle, so the stress increases gradually at the 2nd, 4th, and 6th passes, and decreases at the 9th pass. The plastic strain is related to the increment of forming angle and forming angle, and the strain increases with the increment of forming angle during roll forming. However, according to the actual production, it is found that the better the stability of the edge of the sheet with the increase of thickness, the less likely the defects of products such as edge wave will occur. Therefore, the thicker the sheet, the better the forming effect when the maximum stress is less than the tensile strength of the material in roll forming process.

3.1.3 Effect of material yield strength on sheet forming

Based on FAI.5B, DP780 steel and Q235 steel were selected to study the effect of yield strength of different materials on roll forming when the thickness of sheet was 1.5 mm. The influence of stress and equivalent plastic strain curve of different sheets in bending zone is shown in Fig. 22. The stress of DP780 sheet in roll forming process is much higher than that of Q235. The maximum stress appears in the sixth pass, which is as high as 820 MPa, but it does not exceed the tensile limit of the sheet. Although DP780 sheet is subjected to strong stress, its maximum plastic strain is only 0.124, which is lower than that of Q235 sheet under the same condition.

3.2 Effect of forming parameters on sheet springback in roll forming

3.2.1 Effect of forming angle distribution method on sheet Springback in roll forming

The Q235 sheet with a thickness of 1.5 mm was simulated in this experiment, and the roll forming changes were studied in the 2nd, 4th, 6th and 9th passes. This experiment focused on the analysis of the stress and strain changes of the sheet without unloading the load (before springback) after complete forming and after unloading the load (after springback). Fig. 23 shows the stress and equivalent plastic strain nephograms of the roll forming parts before and after springback based on FAI.5B.

As can be noticed from Fig. 23, the maximum stress and plastic strain of the sheet after complete forming (without unloading load, before springback) based on FAI.5B are 5 MPa and 0.01 lower than those of the sheet in the forming process illustrated in Figs. 10 and 12, respectively. This is because the stress of sheet forming is not only affected by this pass, but also by other passes. The maximum stress and plastic strain of the sheet after unloading (springback) are 3 MPa and 0.01 lower than those of the sheet after full forming (unloading, springback), respectively.

This is because the internal stress of the sheet is released after unloading, which is also the main reason for springback. It can be seen from the cloud that the maximum stress and strain still occur in the bending zone; hence, springback mainly occurs in the bending zone. The distribution of stress and strain is the same under different forming angle increments; however, their numerical values are different.

When comparing the simulation results for the stress and strain changes before and after springback under three different angular distribution modes, namely, FAI.5B, FAI.4B, and FAI.10°, it was found that the stress and strain release after unloading is the key factor causing springback. Fig. 24 shows the roll forming parts with different forming angle increments. The numbers in Table 6 represent the average values of many tests. Providing that the cross section of roll forming was symmetrical, the bending zone at the connection between the web and flange was chosen to study the springback angle. The experimental equipment is shown in Fig. 6. The experimental measuring tool was a universal energy angular device with an accuracy of 0.02°.

The measured springback angle values were larger than the

Table 6. Springback angle of roll forming products with different FAIs.

Group	FAI.5B	FAI.4B	FAI. 10°
Experiment	1.40°	2.32°	2.58°
Simulation	1.36°	2.22°	2.34°

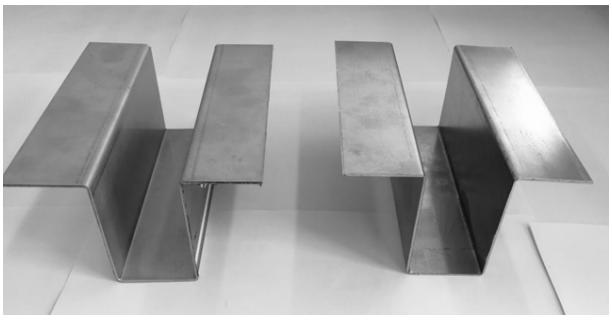

Fig. 24. Roll forming products with different FAIs.

simulated values because the simulated environment was set under ideal conditions, and there were many uncontrollable factors causing sheet springback in the experiment. However, the difference in the springback angle values between the simulation and experiment was very small across the forming modes. This confirms the accuracy of the simulation, which can serve as an important theoretical guideline.

3.2.2 Effect of sheet thickness on sheet springback in roll forming

Figs. 25 and 26 are experimental products with different sheet thickness and different passes.

Based on FAI.5B, the springback angle of each pass of 1.0 mm, 1.5 mm, 2.0 mm and 4.0 mm plate thickness is measured, and Fig. 27 is drawn. Fig. 27 shows the springback curve under different sheet thickness values.

It can be noticed from Fig. 27 that the springback is smaller in the 1st pass and larger in the 2nd, 3rd, and 4th passes. Starting from the 3rd pass, the springback gradually decreases with the increase in the forming pass number. This is because the increment of the forming angle decreases gradually; that is, the springback angle increases with the increase in the forming angle. It can also be found that the springback angle decreases with the increase in the thickness of the sheet. The springback angle is linearly related to the thickness of the sheet, and the change in the thickness of the sheet directly affects the springback angle after bending unloading. The main reason for this effect is that the surface strain and stress of the sheet with a large thickness are larger and the sheet will produce more plastic deformation, which results in the decrease of the springback angle.

3.2.3 Effect of material yield strength on sheet springback in roll forming

The influence of yield strength on sheet springback was studied based on the same parameters such as FAI.5B and

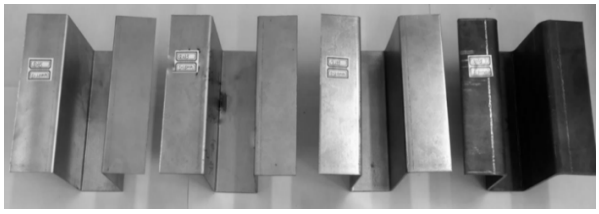

Fig. 25. 1.0 mm, 1.5 mm, 2.0 mm and 4.0 mm products based on FAI.5B.

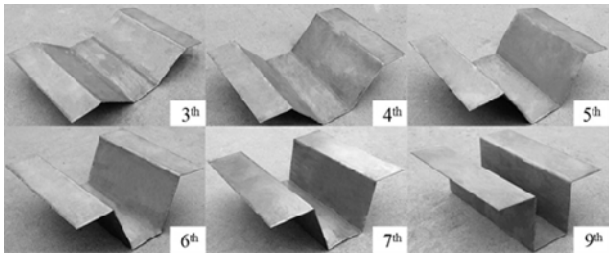

Fig. 26. Third to seventh and ninth experimental products with 1.5 mm.

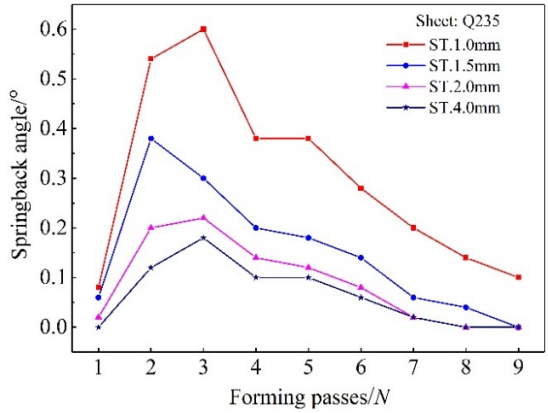

Fig. 27. Springback angle with different sheet thicknesses.

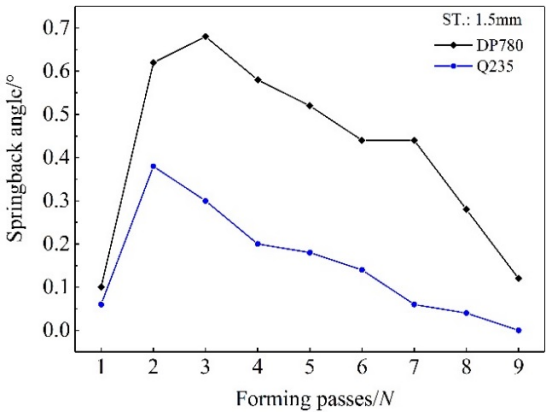

Fig. 28. Springback with different sheet yield strength.

1.5 mm sheet thickness. According to the springback experimental data, the broken line diagrams of the effect of yield strength of different materials on springback were drawn, as shown in Fig. 28.

When the sheet thickness was 1.5 mm, the springback angle

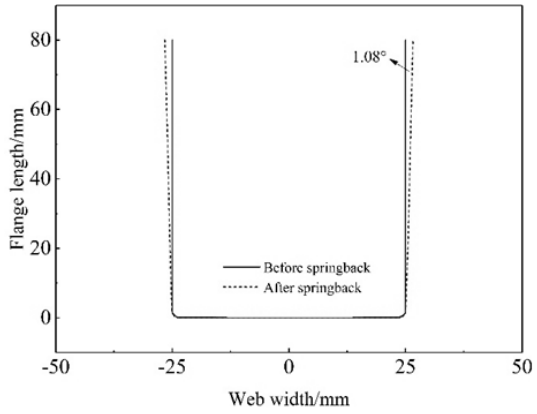

Fig. 29. Springback with correction rolls.

of DP780 was significantly higher than that of Q235, which indicates that the yield strength of the material has a significant impact on the springback angle of the sheet. The greater the yield strength of the material, the more serious the springback is. This is in line with the theoretical guidance and experimental expectations.

3.2.4 Effect of the correct roll compensation on sheet springback in roll forming

Springback is inevitable in sheet forming. However, it can be reduced to achieve higher accuracy of the products. In roll forming manufacturing, in addition to exploring different distributions of the forming angle, more forming passes can be set or the springback compensation of the corrected rolls can be increased to reduce springback. In this study, a set of rolls with the forming angle being the same as in the 9th pass were added, and the springback angle during sheet forming was measured after adding the correction rolls. The measurement results are illustrated in Fig. 29.

It can be noticed from Fig. 29 that the springback angle of the sheet is 1.08° after the correction rolls were added. The springback decreased by 0.28° when the correction rolls were not added. In the actual production process, increasing the number of correction rolls or forming passes can reduce springback well. When adding a correction roll to adjust the forming angle, attention should be paid to the setting of the compensation angle to prevent excessive bending.

4. Conclusions

In this study, the cap-shaped roll-forming parts of small section profiles commonly used in industrial production were taken as the research object. The roll-forming process was investigated and FAI.5B was proposed to address the lack of scientific theoretical guidance on the distribution of the forming angle in roll forming. The effects of the forming angle, sheet thickness, and sheet yield strength on the stress, strain, and springback of a sheet during roll forming were analyzed using an experiment and a simulation implemented in ABAQUS finite element software and. The following results were obtained.

1) The maximum stress and equivalent plastic strain under three different FAIs (FAI.5B, FAI.4B and FAI.10°) were 298 MPa, 340 MPa, 376 MPa and 0.165, 0.26, and 0.295, respectively. Providing that a small stress concentration and plastic strain could reduce defects while not exceeding the material yield strength, the forming angle based on FAI.5B was found to be superior compared to that achieved with other forming methods.

2) During roll forming, the stress and plastic strain in the bending zone of the sheet were much higher than those in the web and flange zones, while the transverse strain in the bending zone was higher than the longitudinal strain. With the increase in the thickness of the sheet, the stress and strain in the bending zone of the sheet increased correspondingly. When roll-forming sheets with different thickness, the distribution and change trend of the stress and strain were consistent. The thicker the sheet was, the better the forming effect was when the maximum stress was less than the tensile strength of the sheet during roll forming.

3) The maximum stress and strain of the sheet after unloading (springback) were less than those before unloading (springback). The maximum stress and strain of the forming angle were reduced by 3 MPa and 0.01 after unloading based on FAI.5B, resulting in a springback angle of 1.40°. However, the springback was the smallest for FAI.5B compared to that for other forming methods. It is concluded that the forming angle based on FAI.5B is superior to that achieved using other FAIs.

4) Based on the research condition of five-boundary condition forming angle distribution function, after roll forming, the springback angle decreased with the increase in the sheet thickness in a linear manner. The springback angle of the sheet also increased with the increment of the forming angle and increase in the material yield strength.

5) It was confirmed that springback can be effectively reduced by increasing the number of passes or correction rolls. In our experiments, the springback angle could be reduced to 1.08° after adding a set of correction rolls.

Acknowledgments

The authors would like to acknowledge the financial support provided by the National Natural Science Foundation of China (Grant No.51305241), National Natural Science Foundation of China (Grant No.51705295), Natural Science Foundation of Shandong Province (CN) (ZR2018MEE022), and Youth Innovation Team Development Plan of Colleges and Universities in Shandong province (2019KJB015).

Nomenclature

N	: The number of forming passes
θ_0	: The final forming angle of the vertical edge
H	: The length of the vertical edge

I : The forming pass number
θ_i : The forming angle
$\Delta\theta_i$: The forming angle increment
FAI : Forming angle increment (distribution method)
FAI.5B : Five-boundary condition forming angle distribution function
FAI.4B : Four-boundary condition forming angle distribution function
FAI.10° : 10° increment of forming angle
S.T. : Sheet thickness
PEEQ : Equivalent plastic strain
S : Stress

References

[1] J. Salem, H. Champliaud, Z. Feng and T. M. Dao, Experimental analysis of an asymmetrical three-roll bending process, *International Journal of Advanced Manufacturing Technology*, 83 (9-12) (2016) 1823-1833.

[2] J. H. Wiebenga et al., Product defect compensation by robust optimization of a cold roll forming process, *Journal of Materials Processing Technology*, 213 (6) (2013) 978-986.

[3] Y. D. Asl, M. Sheikhi, A. P. Anaraki, V. Panahizadeh R. and M. H. Gollo, Fracture analysis on flexible roll forming process of anisotropic Al6061 using ductile fracture criteria and FLD, *International Journal of Advanced Manufacturing Technology*, 91 (5-8) (2016) 1-12.

[4] B. S. Bidabadi et al., Experimental and numerical study of bowing defects in cold roll-formed, U-channel sections, *Journal of Constructional Steel Research*, 118 (2016) 243-253.

[5] J. Jiao, B. Rolfe, J. Mendiguren and M. Weiss, An analytical model for web-warping in variable width flexible roll forming, *International Journal of Advanced Manufacturing Technology*, 86 (5-8) (2016) 1541-1555.

[6] H. S. Park and T. V. Anh, Optimization of bending sequence in roll forming using neural network and genetic algorithm, *Journal of Mechanical Science and Technology*, 25 (8) (2011) 2127-2136.

[7] Y. Yan et al., Finite element simulation of flexible roll forming with supplemented material data and the experimental verification, *Chinese Journal of Mechanical Engineering*, 29 (2) (2016) 342-350.

[8] R. Safdarian and H. M. Naeini, The effects of forming parameters on the cold roll forming of channel section, *Thin-Walled Structures*, 92 (2015) 130-136.

[9] H. Ona, T. Jimma, H. Kozono and T. Nakako, Computer-aided design for cold roll forming of light-gauge steel members, *Trans. Jpn. Soc. Mech. Eng.*, 55 (512) (2008) 1116-1121.

[10] B. S. Bidabadi, H. M. Naeini, M. S. Tehrani and H. Barghikar, Experimental and numerical study of bowing defects in cold roll-formed, U-channel sections, *Journal of Constructional Steel Research,* 118 (2016) 243-253.

[11] B. S. Bidabadi, H. M. Naeini, R. A. Tafti and H. Barghikar, Experimental study of bowing defects in pre-notched channel section products in the cold roll forming process, *International Journal of Advanced Manufacturing Technology*, 87 (1-4) (2016) 997-1011.

[12] Z. W. Han et al., Spline finite strip analysis of forming parameters in roll forming a channel section, *Journal of Materials Processing Tech.*, 159 (3) (2004) 383-388.

[13] C. J. Su et al., Research on roll forming process based on five-boundary condition forming angle distribution function, *International Journal of Advanced Manufacturing Technology*, 102 (9-12) (2019) 3767-3779.

[14] M. Weiss et al., Comparison of bending of automotive steels in roll forming and in a V-die, *Key Engineering Materials*, 504-506 (2012) 797-802.

[15] P. Groche, P. Beiter and M. Henkelmann, Prediction and inline compensation of springback in roll forming of high and ultra-high strength steels, *Production Engineering,* 2 (4) (2008) 401-407.

[16] G. Zeng et al., Numerical simulation and sensitivity analysis of parameters for multistand roll forming of channel section with outer edge, *Journal of Iron and Steel Research International*, 16 (1) (2009) 32-37.

[17] C. J. Su et al., Research on roll-forming bending angle distribution function based on five boundary conditions, *Journal of Mechanical Science and Technology*, 31 (7) (2017) 3445-3453.

Chunjian Su received his M.Sc. (2004) and Ph.D. (2007) in Material Processing Engineering from Yanshan University in China. Now he is a Professor of Mechanical Engineering and Automation at Mechanical and Electronic Engineering Department, Shandong University of Science and Technology. His current research interests include different aspects of artificial intelligence and electromechanical systems.